ELSEVIER

Journal of Nuclear Materials 278 (2000) 358–363

journal of nuclear materials

www.elsevier.nl/locate/jnucmat

Letter to the Editors

Irradiation behavior of U_6Mn–Al dispersion fuel elements

M.K. Meyer [a,*], T.C. Wiencek [b], S.L. Hayes [a], G.L. Hofman [b]

[a] *Argonne National Laboratory – West, P.O. Box 2528, Idaho Falls, ID 83404, USA*
[b] *Argonne National Laboratory – East, 9700 S. Cass Avenue, Argonne, IL 60439, USA*

Received 9 August 1999; accepted 17 November 1999

Abstract

Irradiation testing of U_6Mn–Al dispersion fuel miniplates was conducted in the Oak Ridge Research Reactor (ORR). Post-irradiation examination showed that U_6Mn in an unrestrained plate configuration performs similarly to U_6Fe under irradiation, forming extensive and interlinked fission gas bubbles at a fission density of approximately 3×10^{27} m^{-3}. Fuel plate failure occurs by fission gas pressure driven 'pillowing' on continued irradiation. Published by Elsevier Science B.V. All rights reserved.

1. Introduction

Recently, there has been renewed interest in very high-density dispersion fuel for use in research reactors [1]. Conversion of high power research reactors from HEU (highly enriched uranium) to LEU (low-enriched uranium) requires dispersion fuel with uranium densities of 8000–9000 kg/m^3. Current commercial plate-type dispersion fuel fabrication technologies are not practical for manufacturing fuel at loadings above ~55 vol.%. Given this practical constraint on fuel volume loading, fuel phases with uranium densities of at least 14 500 kg U/m^3 are required to fabricate LEU dispersion fuel using existing methods. Two types of fuel are available that meet this density criterion; metallic uranium of low alloy content, and the U_6Metal class of high-density intermetallics.

The irradiation behavior of U_6Fe plate-type dispersion fuel has been investigated as a candidate high-density fuel. It has been shown to have poor irradiation behavior due to break-away swelling of the fuel phase at low burnup [2]. Limited irradiation studies of U_6Mn were carried out in conjunction with studies of U_6Fe and other fuel materials in the late 1980s. Recent interest in U_6Mn as a candidate dispersion fuel phase [3] has encouraged the publication of observations based on this data.

2. Fuel plate fabrication

2.1. Preparation of U_6Mn

Fuel ingots were prepared by arc melting. Charges were melted, turned, and remelted three or four times. Results from chemical analysis of LEU and MEU (medium enriched uranium) ingots are given in Table 1. The composition was chosen as hyper-stoichiometric with respect to U_6Mn in order to avoid formation of the α-uranium solid solution phase. The uranium–manganese phase diagram [4] indicates that the material should be composed of 91 wt% U_6Mn and 9 wt% UMn_2. X-ray diffraction of the fuel powder showed that the major phase present was U_6Mn. An optical micrograph of the as cast ingot is shown in Fig. 1. Although no micro-chemical information is available, the micrograph shows what appears to be primary U_6Mn phase and a eutectic mixture of U_6Mn and UMn_2. The density of arc-cast alloy ingots, measured by immersion, was 16 800 kg/m^3. The calculated density of a mixture of 91 wt% U_6Mn and 9 wt% UMn_2 is 17 100 kg/m^3, supporting the assumptions about the phase array.

* Corresponding author. Tel.: +1-208 533 7461; fax: +1-208 533 7863.
E-mail address: mitchell.meyer@anl.gov (M.K. Meyer).

0022-3115/00/$ - see front matter.
PII: S0022-3115(99)00280-9

Table 1
Chemical analysis of U_6Mn

Ingot no.	Total U (wt%)	Enrichment (wt% ^{235}U)	Mn (wt%)	O (wt%)	Other (wt. ppm)
E236	93.25	19.79	6.08	0.39	314 Fe + Ni 393 N 9 H
E237	93.32	40.0	6.11	0.14	139 Fe + Ni 107 N 0 H

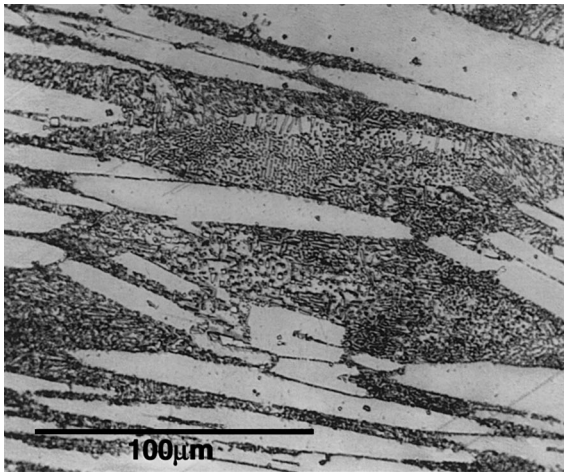

Fig. 1. Optical micrograph of as-cast U_6Mn fuel ingot E-236. Refer to Table 1 for chemical analysis.

2.2. Fabrication of fuel test plates

The LEU and MEU ingots described in Table 1 were used to make fuel powder by manually grinding with a hardened steel mortar and pestle. Fuel powder was mixed with commercial air-atomized aluminum powder, pressed into fuel compacts, placed into 6061 aluminum frames, and hot rolled to produce 11.4×5.08 cm^2 fuel plates. Nominal plate thickness was either 1.27 or 1.52 mm. The fuel fabrication procedure is described in detail in Ref. [5]. The final fuel form is a thin plate consisting of a core (meat) of U_6Mn dispersed in aluminum and clad in aluminum. Attributes of the test plates used for irradiation are given in Table 2. Fuel zone porosity is calculated by subtracting the volume of the fuel plate components from the measured immersion volume. Fuel core thickness was calculated from rolling reduction ratios, while plate thickness values were measured.

The microstructure of an as-fabricated fuel plate (A-226) is shown in Fig. 2. The fuel phase partially reacted with the aluminum matrix during fuel fabrication at 500°C for approximately 2 h. Qualitative EDS shows that the reaction product contains uranium, aluminum, and manganese. The degree and extent of reaction was varied, and the reaction product did not form a uniform interaction layer around fuel particles.

2.3. Irradiation

The fuel plates were assembled into a test module for irradiation in the ORR. The test configuration was similar to that described in Ref. [6]. Miniplates were placed into a module with 2.54 mm coolant channels between each plate. Reactor primary coolant water was used to cool the plates. All test plates were irradiated in the same module (Module 33) at the same time for 146.9 EFPD. The fuel core dimensions were chosen to give approximately the same plate power for both LEU and MEU plates, and fuel plate surface temperatures for both enrichments was estimated to be 110 ± 10°C. Measured or calculated average fission density and ^{235}U burnup for

Table 2
As-fabricated U_6Mn fuel test plate data

Plate no.	Fuel volume loading (%) (V_f)	U loading (g/cm^3)	Enrichment (%)	Fuel zone porosity (%)	Fuel core thickness/plate thickness (mm)
A-225	44.2	6.92	19.79	15.6	0.53/1.24
A-226[a]	45.4	7.12	19.79	13.2	0.53/1.24
A-227	44.0	6.89	19.79	16.0	0.54/1.52
A-228	45.0	7.05	19.79	14.0	0.54/1.54
A-229	39.4	6.18	40.00	15.2	0.31/1.25
A-231	39.7	6.22	40.00	14.7	0.31/1.25
A-232	39.9	6.26	40.00	14.2	0.31/1.28

[a] Not irradiated, sectioned for metallography.

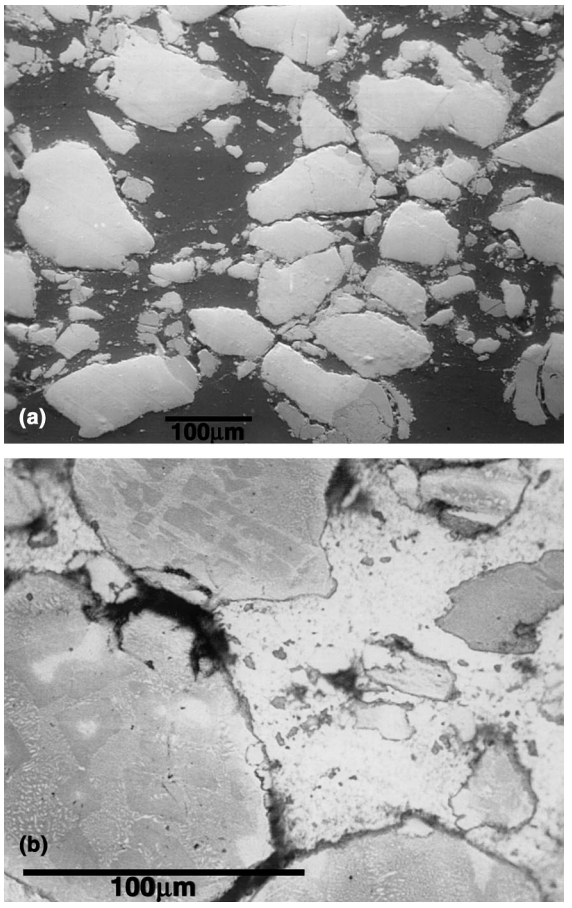

Fig. 2. Microstructure of as-fabricated U_6Mn (plate A-226). (a) SEM. U–Al–Mn reaction phase shows as dark contrast on bright fuel particles. (b) Optical micrograph showing as-fabricated porosity and fuel microstructure.

the fuel are given in Table 3. The fuel core fission density column gives the fission density in the volume of aluminum and U_6Mn that makes up the fuel core; the fuel particle fission density column gives the fission density in the fuel particles themselves. Since they were irradiated for the same length of time at approximately the same reactor power levels, the MEU plates saw approximately twice the fission rate of the LEU plates.

3. Post-irradiation examination

Fuel plates were subjected to thickness measurements and immersion density measurements after irradiation. Plate thickness was measured using a micrometer at nine locations in a rectangular grid on the plate. Average thickness and volume change data are listed in Table 4. Fuel swelling was calculated in the usual manner [7]. In order to more accurately calculate fuel swelling, the amount of as-fabricated porosity remaining after irradiation was estimated. Image analysis was used to measure the area of angular pores at fuel particle–aluminum interfaces. Using this method, it was determined that 3.5% of the as-fabricated porosity remained in the LEU plates after irradiation. It was evident from micrographs of the MEU plates that all porosity introduced during fabrication was consumed by fuel particle swelling.

It seems reasonable to assume, based on similarities between U_6Mn, U_6Fe, and U_3Si [8] data, that the general trends observed as a function of fission density are independent of fission rate. The fuel swelling data for both LEU and MEU U_6Mn are plotted in Fig. 3 as a function of the fission density in the fuel phase, along with data for U_6Fe irradiated under similar conditions. Data for U_6Fe is from LEU fuel plates only. The swelling behavior of the two compounds is similar. In general, both materials exhibit moderate swelling behavior to a certain fission density, after which rapid, break-away swelling occurs. For U_6Mn, the transition to the break-away swelling regime occurs at a fission density near 3.0×10^{27} fissions/m^3. After the onset of break-away swelling, large fuel volume changes occur for small increases in fission density. The volume change in MEU plate A-232 was large enough to cause delamination of the fuel plate at an average fission density of 3.9×10^{27} fissions/m^3.

Table 3
Fission density and burnup of irradiated U_6Mn miniplates

Plate no.	Enrichment (%)	^{235}U burnup (avg. %)	Fuel core fission density (10^{27} m^{-3})	Fuel particle fission density (10^{27} m^{-3})	Average fuel fission rate (m^{-3} s^{-1})
A-225	19.79	32.0	0.98	2.21	1.74×10^{20}
A-227	19.79	26.6[a]	0.80	1.83	1.44×10^{20}
A-228	19.79	27.0	0.83	1.86	1.47×10^{20}
A-229	40.00	27.0	1.46	3.72	2.93×10^{20}
A-231	40.00	28.3	1.55	3.90	3.07×10^{20}
A-232	40.00	28.3[a]	1.55	3.90	3.07×10^{20}

[a] Measured value.

Table 4
Post-irradiation thickness and volume measurements

Plate no.	Average thickness (mm)	Thickness change (avg.%)	Core volume change, ΔV_c (%)	Fuel volume change, ΔV_f (%)
A-225	1.30	5.5	−1.3	24.4
A-227	1.58	3.8	−2.7	22.3
A-228	1.63	5.9	−0.9	21.4
A-229	1.54	22.7	38.8	136.9
A-231	1.73	38.7	–[a]	–
A-232	1.63	27.5	110[b]	311

[a] Not measured.
[b] Plate damaged slightly during removal from capsule, data includes the effects of this damage.

Plates A-227 and A-232 were sectioned and metallographically examined using optical and scanning electron microscopy (SEM). Low-burnup LEU plate A-227 is shown in Fig. 4(a); Figs. 4(b) and (c) show cross-sections of opposite ends of plate A-232. Measured burnup for A-232 was 28.0% ^{235}U in the center regions between the areas shown in Fig. 4(b) and (c) with a gradient in burnup along the length of each plate estimated to be ±3% [2]. SEM samples were prepared from plates A-227 and A-232 by punching out a small section of the fuel plate and fracturing the punching through the fuel core, parallel to the cladding surface.

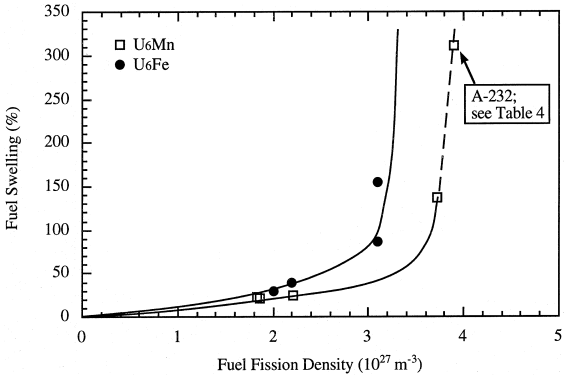

Fig. 3. Fuel particle swelling (ΔV_f) as a function of fission density in the fuel particles for U_6Mn (open points) fuel test plates. U_6Mn data are from both LEU and MEU fuel plates. U_6Fe data are shown for comparison (filled points).

The progression of fission gas driven 'pillowing' with increasing fission density can be seen in Figs. 4 and 5. The microstructure of low-burnup plate A-227 (Figs. 4(a), 5(a) and 6(a)) shows agreement with thickness and immersion density measurements in that there is no gross fuel swelling at the fission density accrued by this plate. SEM (Fig. 6(a)) shows that fission gas bubbles are small and distributed bimodally; similar in behavior to U_3Si and U_6Fe [9]. There are few large gas bubbles within the fuel particles. Remnants of angular porosity from the fuel fabrication process can be seen at the fuel–aluminum interface. At the higher fission densities experienced by A-232, large gas bubbles are present and are beginning to link with adjacent bubbles. Figs. 4(b), 5(b) and 6(b) show areas of the fuel plate in the early stages of break-away swelling. As the fission gas bubbles interlink, fuel particles begin to swell. The swelling at this point is sufficient to fill fabrication pores and to cause some fuel particles to

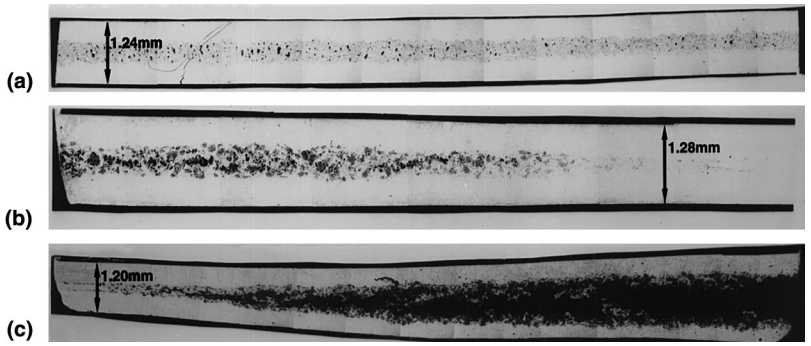

Fig. 4. Low magnification optical images of U_6Mn fuel zone cross-sections. (a) Cross-section of LEU plate A-227, average fuel particle fission density of 1.83×10^{27} m^{-3}. (b) Cross-section of MEU plate A-232 that shows plate structure in the early stages of break-away swelling. (c) Section of MEU plate A-232 that shows delamination occurring in the later stages of break-away swelling.

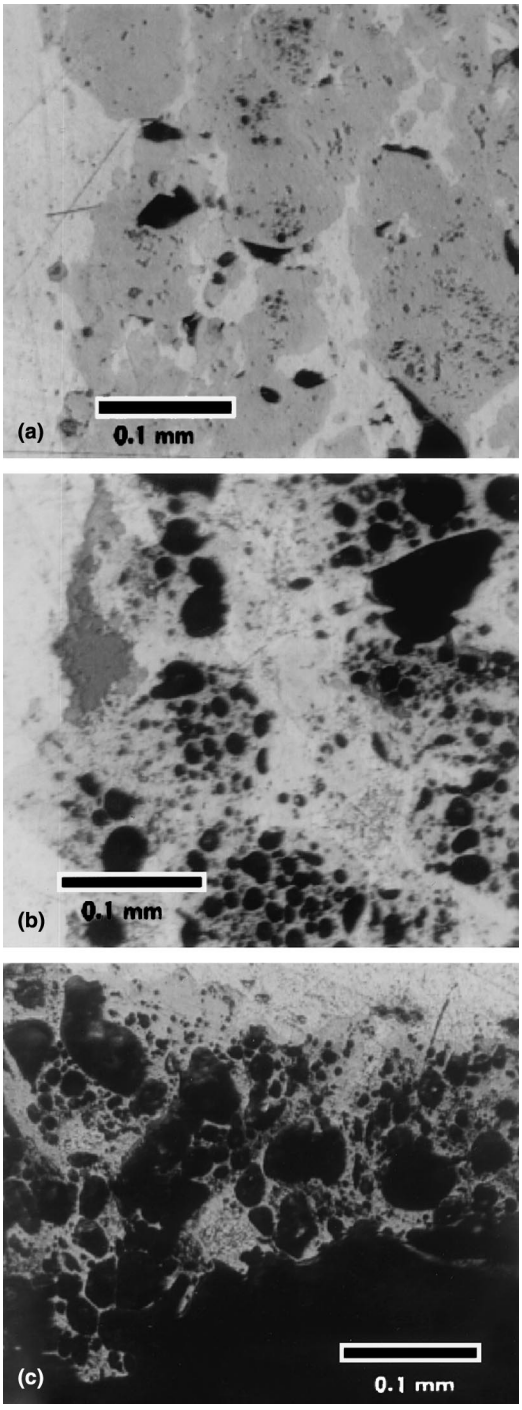

Fig. 5. Optical micrographs of U_6Mn fuel. Areas shown correspond to those in Fig. 4. (a) LEU plate A-227, average fuel particle fission density 1.83×10^{27} m^{-3}. (b) Area of MEU plate A-232 that shows microstructure early in break-away swelling. (c) Section of MEU plate A-232 that shows microstructure after break-away swelling has occurred.

make contact. The angular particle morphology produced by the fuel particle communition process is no longer evident. As bubble interlinking continues (Figs. 4(c) and 5(c)), adjacent fuel particles make contact and large gas pockets form due to inter-particle linking of the gas bubbles. The enhanced gas bubble interlinking and growth behavior in compounds of this type has been ascribed to fission induced amorphization, and the enhanced gas mobility and plastic flow rates that are thought to accompany amorphization [8]. As bubbles interlink and grow, the bubble radius effectively increases. The total volume required to contain a given mass of fission gas increases as the average gas bubble size increases. The thin aluminum cladding provides little mechanical restraint in opposition to this gas volume increase, and fission gas driven pillowing of the plates occurs.

The effect of the two-phase microstructure of the as-cast fuel on the swelling behavior is difficult to ascertain. It is not evident from the post-irradiation micrographs that this structure remains after irradiation. It is possible that both phases transformed to a homogeneous [8,9], amorphous U–6 wt% Mn phase during irradiation.

4. Conclusion

The irradiation behavior of U_6Mn–Al plate-type dispersion fuel is similar to that of U_6Fe. Detectable fission gas bubbles begin to form at low burnup. These bubbles grow and link together to form large gas pockets with increasing burnup. In the absence of appreciable cladding restraint, fission gas pressure causes break-away swelling to begin at a fission density of approximately 3.0×10^{27} m^{-3} for the geometry, fission rates, and fuel loadings studied here. Typical medium power materials test reactors (MTRs) such as the ORR and High Flux Reactor (HFR, Petten, The Netherlands) require fuels that are stable to fission densities of at least 4×10^{27} m^{-3} (55 at.% LEU burnup).

Acknowledgements

This work was supported by the US Department of Energy under contract W-31-109-Eng-38. This work was performed under the supervision of the late R.F. Domagala. The authors would like to thank J.L. Snelgrove for his assistance and comments and L.A. Neimark, R.V. Strain and the staff of the ANL alpha–gamma hot cell for performing the post-irradiation exam.

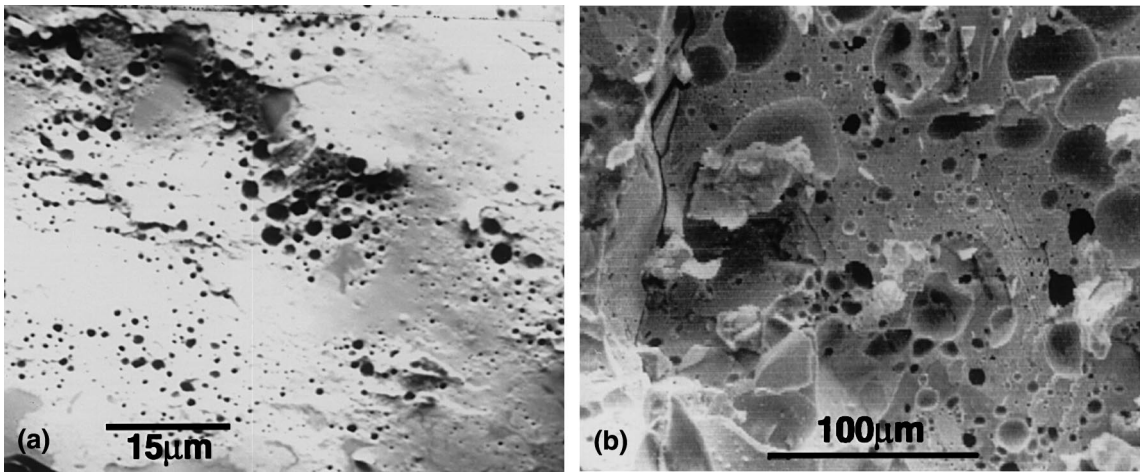

Fig. 6. SEM micrographs of fuel fracture cross-sections. (a) LEU plate A-227, average fuel particle fission density 1.83×10^{27} m^{-3}. (b) MEU plate A-232, same general area shown in Figs. 4(b) and 5(b).

References

[1] J.L. Snelgrove, G.L. Hofman, M.K. Meyer, C.L. Trybus, T.C. Wiencek, Nucl. Eng. Des. 178 (1997) 119.
[2] G.L. Hofman, R.F. Domagala, G.L. Copeland, J. Nucl. Mater. 150 (1987) 238.
[3] M. Ugajin, A. Itoh, M. Akabori, N. Ooka, Y. Nakakura, J. Nucl. Mater. 254 (1998) 78.
[4] M. Hansen, K. Anderko, Constitution of Binary Alloys, 2nd Ed., Genium Publishing, 1985, p. 960.
[5] T.C. Wiencek, Summary report on fuel development and miniplate fabrication for the RERTR program, 1978–1990, ANL/RERTR/TM-15, 1995.
[6] R.L. Senn, M.M. Martin, Irradiation testing of miniature fuel plates for the RERTR program, ORNL/TM-7761, 1981.
[7] G.L. Hofman, Y. Fanjas, in: Proceedings of the 16th International Meeting on Reduced Enrichment for Research and Test Reactors, JAERI-M 94-042, Japan Atomic Energy Research Institute, 1994, p. 159.
[8] G.L. Hofman, J. Nucl. Mater. 140 (1986) 256.
[9] J.R. Rest, G.L. Hofman, R.C. Birtcher, in: 14th International Symposium, ASTM STP 1046, 1990, p. 789.